ELSEVIER

Solid State Ionics 150 (2002) 263–279

SOLID STATE IONICS

www.elsevier.com/locate/ssi

Resolution of conflicting views concerning frequency-response models for conducting materials with dispersive relaxation, and isomorphism of macroscopic and microscopic models

J. Ross Macdonald *

Department of Physics and Astronomy, University of North Carolina, Chapel Hill, NC 27599-3255, USA

Received 11 September 2000; received in revised form 12 February 2002; accepted 12 March 2002

Abstract

Possible errors in the widely used 1972–1973 macroscopic original-electric-modulus formalism are identified, corrected, and their consequences considered. These errors include misidentification of the high-frequency-limiting dielectric constant arising entirely from mobile charges, $\epsilon_{C1\infty}$, and the failure to treat properly the high-frequency-limiting dielectric constant associated with bulk dipolar and vibrionic effects, $\epsilon_{D\infty}$. It is shown that the corrected modulus formalism, which describes dispersed mobile-charge effects, is isomorphic in form with the 1973 microscopic continuous-time random-walk hopping model of Scher and Lax after a minor but significant correction is made to the latter's response function. This firmly established correction, which nevertheless could not be determined by Kronig–Kramers transformation, involved inversion of synthetic frequency-response data to determine a distribution of relaxation times and led to extension of the real part of the Scher–Lax dielectric response to higher frequencies by the inclusion of a nonzero limiting value. This isomorphism, along with excellent data fitting using the corrected modulus formalism, suggests that since the Scher–Lax stochastic model involves no explicit Coulomb interactions, cation motion in glasses is dominated by short-range interactions. Finally, two very-high-frequency processes, which each lead to a limiting plateau value of the real part of the conductivity at sufficiently high frequencies, are discussed in detail.
© 2002 Elsevier Science B.V. All rights reserved.

PACS: 72.20.−i; 66.10.Ed; 77.22.Gm; 81.05.Kf
Keywords: Conductivity relaxation; Electric modulus formalism; Kohlrausch–Williams–Watts; Stretched-exponential; Immittance-spectroscopy data fitting; Disordered materials; Ionic glasses

1. Introduction and background

1.1. General

Electrical relaxation measurements, particularly in the frequency domain, immittance spectroscopy (IS), are widely used to help characterize the dynamics of diffusing charges in glasses, melts, and single crystals [1]. For example, see references 1–33 of Ref. [2]. Nevertheless, there seem to remain endemic problems of data interpretation, some of them addressed and resolved herein. Although I shall be primarily concerned with ionic motion in disordered materials, many of the results are of broader applicability. A list of acronym definitions appears at the end of this work.

* Tel.: +1-919-967-5005; fax: +1-919-962-0480.
E-mail address: macd@email.unc.edu (J.R. Macdonald).

0167-2738/02/$ - see front matter © 2002 Elsevier Science B.V. All rights reserved.
PII: S0167-2738(02)00525-8

As is well known, there are four closely related levels at which a frequency response model or experimental data may be expressed and a model fitted to the data. In terms of specific model quantities, these are the complex dielectric constant, $\epsilon(\omega) = \epsilon'(\omega) - i\epsilon''(\omega)$; the complex conductivity, $\sigma(\omega) \equiv i\omega\epsilon_V\epsilon(\omega) \equiv 1/\rho(\omega) \equiv i\omega\epsilon_V/M(\omega) = \sigma'(\omega) + i\sigma''(\omega)$; the complex resistivity, $\rho(\omega) \equiv 1/\sigma(\omega) = \rho'(\omega) + i\rho''(\omega)$; and the complex electric modulus, $M(\omega) \equiv i\omega\epsilon_V\rho(\omega) \equiv 1/\epsilon(\omega) = M'(\omega) + iM''(\omega)$. Here ϵ_V is the permittivity of vacuum.

In the following, some discussion of the differences between conductive-system and dielectric-system dispersion responses is presented along with some necessary definitions. Then, two important frequency-response conductive-system models are defined and discussed: the original and the corrected modulus formalisms. It is next shown what needs to be done to produce full response isomorphism between an important microscopic hopping model and the macroscopic one generally used as the basis of the modulus formalisms. A discussion of very-high-frequency effects follows, and then a summary is presented of the important differences between the two modulus formalism models.

1.2. Differences in conductive and dielectric responses

When one deals with a single dispersive process associated only with mobile charges, defined as conductive-system dispersion (CSD), as will be the case herein, we may write its full $\rho(\omega)$ response in general terms as

$$\rho(\omega) = \rho'(\infty) + \{\rho'(0) - \rho'(\infty)\}I(\omega), \qquad (1)$$

where $I(\omega)$ is a normalized, complex macroscopic response function for which $I'(0) = 1$ and $I'(\infty) = 0$. Where needed, a subscript 'C' will be included to designate conductive-system model quantities, and a subscript 'D' employed for dielectric ones. For CSD, unlike dielectric-system dispersion (DSD), the dc and ac responses are closely related [3–9].

With a plausible dispersion model for $I(\omega)$, one finds that the $\rho(\omega)$ response of Eq. (1), expressed at the complex dielectric constant level, involves $\epsilon'_C(\omega)$ dielectric response arising solely from mobile charges, response whose high-frequency limit may or may not be zero, depending on the details of the $I(\omega)$ model [4,5]. Because all real data include dielectric response as well, often well approximated for dominant CSD situations by a frequency-independent dielectric constant, $\epsilon'_D = \epsilon_{D\infty}$, the effect of this quantity must always be included in any full response model. Such a model then involves CSD and DSD response functions in parallel electrically; see, for example, Fig. 1 of Ref. [7].

For conductive-system dispersion, $I(\omega)$ is usually defined at the complex resistivity level in terms of a distribution of resistive relaxation times (DRT), τ_C, but its response may be transformed to any of the other three levels. In particular, the same DRT leads to response expressed at either the complex resistivity level, as in Eq. (1), or at the modulus level, and the DRT may be estimated by inversion of data at any of the four immittance levels, as illustrated later. An example of peaked $\rho''(\omega)$, $M''(\omega)$, and $\epsilon''(\omega)$ responses calculated from the same data appears in Fig. 2 of Ref. [7] and illustrates their different shapes. Note that we may always define and estimate a single, unique CSD DRT from response expressed at either the complex resistivity level or at the modulus level.

However, this is not the end of the story. One can also describe IS response data by means of a distribution of dielectric relaxation times, appropriate for DSD. When such a distribution is known, it is most appropriate to use it to generate or analyze data at the complex dielectric constant level or at the admittance level. In a dielectric situation, the response arises primarily from dielectric dispersion and may or may not involve a nondispersed parallel conductivity that is not a part of the dielectric dispersion and is unrelated to the characteristic dielectric relaxation time of the response, τ_{Do}.

Here again, response associated with the dielectric DRT may be expressed at any of the four immittance levels. However, it is important to note that even when a CSD DRT and a DSD DRT are taken of exactly the same form, their frequency responses are different and involve different temperature dependencies. Nevertheless, it turns out that one can often fit synthetic CSD data with a DSD model and vice versa, provided the DSD response model involves a parallel conductivity element [6]. Good CSD-model fitting of DSD data sometimes requires a nonphysical negative value

of the parallel conductivity, however. Even when both CSD and DSD fits of an experimental data set yield equivalently good results, one can still decide whether the observed dispersion is of CSD or DSD character by comparison of results for a range of fitting temperatures. It appears that some past work has introduced a dielectric DSD for modeling experimental data when a CSD response model would have been more appropriate; for example, see Ref. [10].

1.3. High-frequency-limiting dielectric quantities

As usual, we consider a thermally activated conductive-system, one that involves a nonnegligible dc conductivity, $\sigma_0 \equiv \sigma'(0)$, associated with mobile charges such as ions and given by the zero-frequency limit of the $\sigma(\omega)$ function following from a dispersive response model. Because the matter is often ignored, it is important to distinguish specific model quantities from expressions meant to represent experimental data directly. Where appropriate, a subscript 'E' will be used to denote such latter quantities. In addition, a subscript 'dat' will be used when needed with symbols representing experimental data.

It has been conventional to designate high-frequency-limiting quantities by a symbol or subscript of ∞. Of course, this usage does not mean that such quantities are actually frequency-independent from some particular frequency up to $\omega = \infty$, and it should only be interpreted as indicating approximate constancy up to frequencies that extend at least to the limit of the available experimental range. For example, when there is negligible bulk-material dipolar/vibrionic dielectric relaxation within the full frequency range explored, we set, for that range, $\epsilon'_D(\omega) = \epsilon'_D(0) = \epsilon'_D(\infty) \equiv \epsilon_{D\infty}$, a quantity always >1. Then, in the absence of electrode effects, the only significant dispersion present in the experimental range will be of conductive-system character.

In recent years, the important distinction between $\epsilon_{D\infty}$ and $\epsilon'_E(\infty) \equiv \epsilon_\infty$, discussed below, has largely been ignored, and ϵ_∞ has been employed when it seems that $\epsilon_{D\infty}$ was meant. Even worse, effects of $\epsilon_{D\infty}$ have frequently been ignored or treated incorrectly. See below and Refs. [3–9] for discussions of the problem. Particularly important is the misleading use of the symbol ϵ_∞ in situations where $\epsilon_\infty \neq \epsilon_{D\infty}$ yet the two quantities are not distinguished from each other. As demonstrated herein and earlier [3–9], the neglect or improper treatment of $\epsilon_{D\infty}$ in immittance spectroscopy data analysis, can, and usually does, lead to serious errors in the interpretation of experimental $M''_E(\omega)$ data and plots. Further, Ngai and Rendell [2] have stated that the contributions of mobile ions to $\epsilon'(\omega)$ are seldom considered. As we shall see in Section 3, this contribution has indeed been considered since at least 1994 [3–5], and it is crucial in distinguishing between the original electric modulus formalism (OMF) fitting model [11–13] and its corrected version [3–8]. Further discussion of modeling the high-frequency behavior of $\epsilon'_C(\omega)$ and $\sigma'_C(\omega)$ is presented in Sections 4.2 and 5.

2. Conductivity or modulus level analysis?

When the electric modulus has been discussed and used in the past, it has generally involved presenting data by means of a plot of $M''_{dat}(\omega)$ vs. the logarithm of frequency. Such plots show peaked response, and that to the left of the peak decreases rapidly, minimizing the influence of any low-frequency electrode effects present in data. However, just because such effects are suppressed in $M''_{dat}(\omega)$ plots does not mean that they make a negligible contribution to the data, as is often asserted [11–13], and so one must not assume their absence but instead use other approaches to identify and quantify them [4–8]. In discussing the choice between $M''(\omega)$ and $\sigma'(\omega)$ for data analysis, Roling has recently said, "In the literature, it is highly controversial how these electrical properties should best be analyzed" [14]. See, for example, references 3–11 in Ref. [14].

An advantage of the use of $\sigma'(\omega)$ for comparison between data and models is that $\sigma'_C(\omega) = \sigma'_E(\omega)$, since virtually all bulk capacitative effects appear in $\sigma''_C(\omega)$, but such separation does not occur for the real or imaginary parts of either $M(\omega)$ or $\rho(\omega)$. A frequent error in the literature has been to compare $M''_C(\omega)$ model results, usually denoted by just $M''(\omega)$, with $M''_{dat}(\omega)$, which includes full $M''_C(\omega)$ response as well as the effects of nonzero $\epsilon_{D\infty}$, a quantity that may be greater or smaller than $\epsilon'_C(\infty)$. Of course, the proper comparison should be between $M''_{dat}(\omega)$ and $M''_E(\omega)$, as first emphasized in Ref. [4]. If we fit $\sigma_{dat}(\omega) = i\omega\epsilon_V / M_{dat}(\omega)$ data with $\sigma_E(\omega) = i\omega\epsilon_V[\{M_C(\omega)\}^{-1} + \epsilon_{D\infty}] =$

$i\omega\epsilon_V/M_E(\omega)$ model results, then a correct comparison may be readily made in the absence of electrode effects. It should be noted that this procedure leads to fit results [4–8] that show much less of the endemic high-frequency disparity between data and model observed when proper account is not taken of $\epsilon_{D\infty}$ [11,13,15,16].

The controversy over which analysis approach to use disappears when one realizes that it is most appropriate to fit the real and imaginary parts of a complex data set together to a response model, both to average out some noise and to test directly whether the data set satisfies the Kronig–Kramers relations. Such fitting, which can be done at any of the four IS levels using weighted complex nonlinear least squares (CNLS), should include $\epsilon_{D\infty}$ as a free fitting parameter, as discussed below, and it is readily carried out using the freely available fitting/inversion computer program LEVM [17].

3. Original and corrected electric-modulus-formalism response models

3.1. The original modulus formalism

The original CSD electric modulus formalism, a ground-breaking treatment of bulk conductivity relaxation effects, was developed by Macedo, Moynihan, and their coworkers in 1972–1973 [11–13]. Although it has been shown in the last 6 years that it is inconsistent [3–6], data analysis continues to this day to employ this faulty approach. See, for example, the 20 references to such work in Ref. [18], as well as many others. Luckily, the OMF can be readily corrected, and, as demonstrated herein, the corrected version, the CMF, is important not only because it fits much data for disordered materials much better than does the OMF and many other response models, but also because it can be shown to yield the same frequency response behavior as an important microscopic theory, as discussed below and in Ref. [19], thereby underlining the generality and value of the common response model.

The physical basis of the macroscopic OMF involved consideration of the decay of the electric field in the material at constant displacement, represented by a temporal relaxation function $\Phi_{OMF}(t)$ [13]. The OMF response model was actually implemented by transforming a given distribution of resistivity relaxation times (DRT), $g_C(\tau)$, to a new one proportional to $\tau g_C(\tau)$ [4,5], although no such new distribution was actually defined. In order to distinguish between the two different frequency responses associated with these distributions, I shall use subscripts $k=0$ and 1, respectively [5,7,8,19,20]. Thus, there are two related CSD responses; call them CSD0 and CSD1. Now let $x \equiv \tau/\tau_{ok}$, where τ_{ok} is a characteristic relaxation time of the response. Then the normalized distribution of resistivity relaxation times, $G_{Ck}(x)$, is given by $\tau_{ok}g_{Ck}(\tau)$, and I shall omit the k and 'C' subscripts from now on for $\sigma_0 \equiv \sigma'_C(0)$. Note that the two DRTs lead to the two different $I(\omega)$ responses, $I_0(\omega)$ and $I_1(\omega)$, and so through Eq. (1) to different overall frequency responses.

Next, an important distinction needs to be made: that between consideration of data or a response function expressed at the modulus level and the electric modulus formalism itself. Although the latter was originally derived as a modulus-level response function, it can be transformed to any other immittance level [5]. Thus, the modulus formalism is not equivalent to expressing or considering data or a model at the modulus level, although this distinction has not always been maintained, and the modulus formalism should not be referred to by the ambiguous terms electric modulus or EM [18,21,22].

At the complex resistivity level, the normalized frequency-response functions of Eq. (1), $I_k(\omega)$, may be written as [4,5,19,20]

$$I_k(\omega) = \int_0^\infty \frac{G_k(x)\mathrm{d}x}{[1+i\omega\tau_{ok}x]} = \int_0^\infty \exp(-i\omega t)\{-\mathrm{d}\Phi_k(t)/\mathrm{d}t\}\mathrm{d}t, \qquad (2)$$

showing that $I_k(\omega)$ may be calculated either from knowledge of $G_k(x)$ or from a temporal response function $\Phi_k(t)$, with $\Phi_0(t)$ often called the correlation or autocorrelation function. It involves t/τ_{o1}, and for the OMF $\Phi_0(t)$ is the electric field decay function mentioned above [13]. Through Eq. (2) with $k=0$, $\Phi_0(t)$ leads to the normalized response $I_0(\omega)$, a quantity designated as $N^*(\omega)$ in Ref. [13].

It is important to note that OMF response is *not* that of $I_0(\omega)$, but instead it may be identified with

$I_1(\omega)$ response, one that is readily derived from $I_0(\omega)$ because of the connection between $G_0(x)$ and $G_1(x)$ already mentioned [4,5,13]. Although OMF response was originally derived at the modulus level, and so was later identified as the modulus formalism, its frequency response can be represented at any of the four immittance levels since it involves the same $G_1(x)$ distribution. Derivation of the OMF at the modulus level is fully consistent with that involving Eqs. (1) and (2), and so OMF frequency response may be calculated for any of the immittance levels.

Although the quantity $\rho'(\infty)=\rho'_{Ck}(\infty)\equiv\rho_{Ck\infty}$ appears in Eq. (1) and leads to a high-frequency plateau in $\sigma'(\omega)$, many experimental data sets do not extend to sufficiently high frequencies for a plateau to appear. Further, the OMF, CMF, and many other fitting models do not usually include such response. Therefore, for much of the present work, we set $\rho_{Ck\infty}=0$ but discuss the consequences of $\rho_{Ck\infty}\neq 0$ in Section 5. The mth moments of the normalized $G_k(x)$ distribution are given by

$$\langle\tau^m\rangle_k\equiv\tau_{ok}^m\langle x^m\rangle_k\equiv\tau_{ok}^m\int_0^\infty x^m G_k(x)\mathrm{d}x, \tag{3}$$

and we may also express the first moment, or mean value of τ for the $k=0$ situation, as [23]

$$\langle\tau\rangle_0=\int_0^\infty t\{-\mathrm{d}\Phi_0(t)/\mathrm{d}t\}\mathrm{d}t=\int_0^\infty\Phi_0(t)\mathrm{d}t. \tag{4}$$

Note that $<x^m>_k$ is a dimensionless quantity that depends only on the shape of the distribution and is independent of τ_{ok}.

The OMF analysis [11–13] led to the CSD1 relations

$$M_{\mathrm{OMF}}(\omega)=M_\infty\{1-I_0(\omega)\}, \tag{5}$$

and

$$\sigma_{\mathrm{OMF0}}=\epsilon_{\mathrm{V}}\epsilon_{\mathrm{s}}/\langle\tau\rangle_{\mathrm{OMF}}=\epsilon_{\mathrm{V}}\epsilon_{\mathrm{s}}/\tau_{\mathrm{OMF}}\langle x\rangle, \tag{6}$$

with $M_\infty\equiv M_{\mathrm{OMF}}(\infty)=1/\epsilon_{\mathrm{s}}$, where ϵ_{s} was defined as containing "all the ordinary contributions to the relative permittivity of the material except those connected with the long range ionic diffusion process." [11]. Therefore, it may be identified as the present purely dielectric quantity $\epsilon_{\mathrm{D}\infty}$. Later, it has been denoted by ϵ_∞ but still implicitly or explicitly taken by all users of the OMF to mean $\epsilon_{\mathrm{D}\infty}$ since this quantity has been used in place of the purely conductive-system quantity $\epsilon_{\mathrm{C1}\infty}$, here denoted by $\epsilon_{\mathrm{C1}\infty}$. Its existence means that $\epsilon_{\infty\mathrm{E}}=\epsilon_\infty$ is actually composed of $\epsilon_{\mathrm{C1}\infty}+\epsilon_{\mathrm{D}\infty}$ for CSD1 fitting where $\epsilon_{\mathrm{C1}\infty}$ is nonzero, as it is for data analyzed by the CMF approach for situations where it is a good approximation to take $\rho_{Ck\infty}$ negligible or zero. Further discussion of the important quantity $\epsilon_{\mathrm{C1}\infty}$ appears in (Sections 3.2, 4.2, and 5).

In recent work, Ngai and León [18] state, "This dependence of τ_{EM} (the present τ_{OMF}) on ϵ_∞ is considered by some workers (no references provided) as a shortcoming of the EM formalism. We do not agree with this opinion because this invariably will occur in any representation of the electrical relaxation data because the latter are from macroscopic measurements where ϵ_∞ inevitably enters." First, as one of the "some workers," my position is that the presence of ϵ_∞ $(=\epsilon_{\mathrm{s}}=\epsilon_{\mathrm{D}\infty})$ in the OMF equations is not just a shortcoming but an error in principle. Although the effects of $\epsilon_{\mathrm{D}\infty}$ are indeed always present in the data [4–8], they should not appear directly in a purely CSD model but are, of course, properly included in the fitting of such a model to the data by *adding* an $i\omega\epsilon_{\mathrm{V}}\epsilon_{\mathrm{D}\infty}$ term to a CSD expression for $\sigma_{\mathrm{C}}(\omega)$ to form $\sigma_{\mathrm{E}}(\omega)$. In contrast, since the OMF already includes $\epsilon'_{\mathrm{OMF}}(\infty)=\epsilon_{\mathrm{D}\infty}$ in its response equations, no separate $\epsilon_{\mathrm{D}\infty}$ free fitting parameter has ever been included in OMF fits of experimental data, and the OMF is evidently not expected to require any such added term. Further, it cannot properly define ϵ_∞ as $\epsilon_{\mathrm{C1}\infty}+\epsilon_{\mathrm{D}\infty}$ because the erroneous identification $\epsilon'_{\mathrm{OMF}}(\infty)\equiv\epsilon_{\mathrm{D}\infty}$ preempts the proper $\epsilon_{\mathrm{C1}\infty}\equiv\epsilon'_{\mathrm{C1}}(\infty)$ definition.

Finally, it is worth noting that the OMF Eq. (6) sets stringent and unrealistic conditions on τ_{OMF}. It is not an independent quantity in, for example, Eqs. (2)–(4), but instead it is required be consistent with Eq. (6) and so it depends on $\epsilon_{\mathrm{D}\infty}$ as mentioned above. This problem is avoided when the OMF is corrected in the manner described below.

3.2. The corrected modulus formalism

Here we consider the usual situation where $\epsilon_{\mathrm{C1}\infty}$ is nonzero; but a situation where $\epsilon'_{\mathrm{C1}}(\omega)$ may approach zero, possibly even within the experimental frequency range, is discussed in Section 5. The OMF expres-

sions of Eqs. (5) and (6) are erroneous because the OMF treated a purely conductive-system, dispersive-relaxation situation in terms that include separate conductive *and* dielectric physical processes, as discussed above. Corrected versions of Eqs. (5) and (6) are [4,5]

$$M_{C1}(\omega) = M_{C1}(\infty)\{1 - I_{C0}(\omega)\}, \tag{7}$$

with $M_{C1}(\infty) = 1/\epsilon_{C1\infty}$ and

$$\sigma_{01} \equiv \sigma_0 = \epsilon_V \epsilon_{C1\infty}/\langle\tau\rangle_{01} = \epsilon_V \epsilon_{C1\infty}/\tau_{o1}\langle x\rangle_{01}. \tag{8}$$

These equations do indeed involve only mobile-charge-related quantities. Further, unlike the presence of $\epsilon_{D\infty}$ in Eq. (6) of the OMF, $\epsilon_{C1\infty}$ is a creature of the conductive system only, and it exists only through its definition in Eq. (8) and its presence in model response as $\epsilon'_{C1}(\infty)$. Thus, Eq. (8) imposes no direct restrictions on σ_0, τ_{o1}, or on the relations between them. Their experimental values, and that of $<x>_{01}$, entirely determine the value of $\epsilon_{C1\infty}$.

Note that Eq. (7) shows that although CMF response may be calculated from knowledge of the $k=0$ dimensionless frequency-response function $I_{C0}(\omega)$, it leads to $k=1$ CSD1 response, with different frequency, time, and DRT behavior than that of the associated $k=0$ situation. This is why the subscript 01 has been used in Eq. (8) to indicate that although $<\tau>$ is derived from the CSD0 distribution, it involves a $k=1$ shape parameter whose value may be determined by fitting the CSD1 model of Eq. (7) to data.

It follows from Eq. (7) that

$$\epsilon_{C1}(\omega) = \epsilon_{C1\infty}/\{1 - I_{C0}(\omega)\}. \tag{9}$$

Since $I'_{C0}(\infty) = 0$, $\epsilon'_{C1}(\infty) \equiv \epsilon_{C1\infty}$, a consistent result. But how was Eq. (8) derived? If we consider the $\omega \to 0$ limit of

$$\sigma_{C1}(\omega) = i\omega\epsilon_V\epsilon_{C1}(\omega) = \epsilon_V\epsilon_{C1\infty}\{i\omega/\{1 - I_{C0}(\omega)\}\}, \tag{10}$$

using the result that follows from the first part of Eq. (2) with $k=0$ that $\{1 - I_{C0}(\omega)\} \to i\omega <\tau>_{01}$ to first order as $\omega \to 0$, then Eq. (8) immediately follows on defining $\sigma'_{C1}(0)$ as σ_0.

Why is the CMF a purely conductive-system approach rather than a mixed conductive/dielectric one like the OMF? The original creators of the OMF and virtually all users of it since 1973 have completed it by taking for the $I_0(\omega)$ of Eq. (2) the Kohlrausch–Williams–Watts (KWW) model [24,25], one that follows from the choice of a stretched-exponential (SE) temporal response function,

$$\Phi_{01}(t) = R\exp\{-(t/\tau_{o1})^{\beta_{01}}\}, \tag{11}$$

where the stretching (shape) parameter satisfies $0 \le \beta_{01} \le 1$, and $R=1$ in the absence of cutoff of the associated $G_0(x)$ distribution [4,26]. Even though $\Phi_{01}(t)$ is defined at the $k=0$ level and leads directly to KWW0 (hereafter denoted by K0) frequency response with $\beta_{01} = \beta_0$, it also leads through Eq. (7) to $k=1$ frequency response with $\beta_{01} = \beta_1$, and it is therefore appropriate to denote it with both 0 and 1 subscripts. Thus, fitting data with the CMF model involves the KWW1 (hereafter K1) frequency-response model, one whose shape parameter is β_1, not β_0 [5,6,8,20,27]. It has usually been denoted by just β in previous applications of the OMF. The distinction between the two β's is important because the high-frequency-limiting log–log slope of the K1 $\sigma'_{C1}(\omega)$ response is $n=(1-\beta_1)$, while that of the K0 $\sigma'_{C0}(\omega)$ is β_0, and fitting of limited-range experimental data does not usually lead to exact equality between these quantities [5,6,20].

In the range of $0.3 \lesssim \beta_1 \lesssim 0.7$, CNLS fitting of limited-range simulated data shows that the K1 response model fits such K0 data, or vice versa, reasonably well, and the relation $\beta_1=(1-\beta_0)$ is often a good approximation. However, as $\beta_0 \to 1$, K1 fits of K0 data become progressively poorer and the above relation fails badly. In the Debye limit, $\beta_1 \to 0$ and $\sigma'_{C1}(\omega) = \sigma_0$ over the full ω range [20]. Fig. 1 shows K1 fits, using proportional weighting [6–8,17,26], of nearly exact $\beta_0 = 0.9$ K0 synthetic data with $\tau_{o0} = 5 \times 10^{-4}$ s. For the NLS fit of the real-part $\sigma'_{C0}(\omega)$ data, the estimated β_1 value was about 0.27 rather than 0.1, and for the CNLS fit of both parts, $\beta_1 \simeq 0.45$! The two τ_{o1} estimates were about 4.7×10^{-6} and 6.4×10^{-5} s, respectively.

It is pertinent to compare the above CSD1 CMF expressions of Eqs. (7) and (8) with corresponding ones for the CSD0. For most CSD0 fitting models of interest, such as the K0, $\epsilon_{C0\infty}$ is identically zero unless the associated DRT is cut off and is thus zero

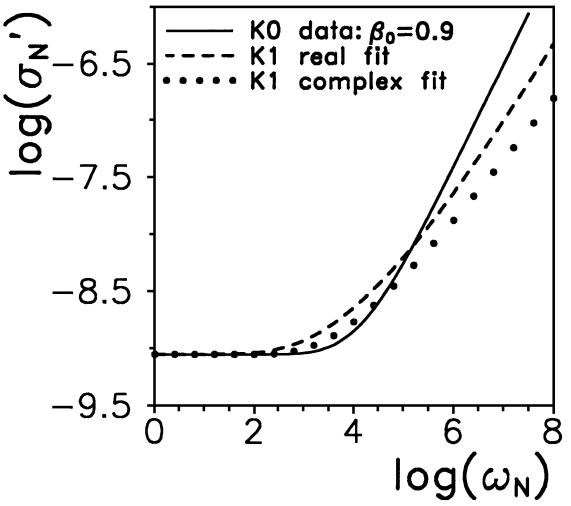

Fig. 1. Dependence of the real part of the complex conductivity on radial frequency for weighted NLS and CNLS fits of accurate $\beta_0 = 0.9$ K0 data using the K1 response model. Here $\sigma_N \equiv \sigma/\sigma_n$, with $\sigma_n = 1$ S/cm, and $\omega_N \equiv \omega/\omega_n$ where $\omega_n = 1$ r/s.

below a nonzero small τ_{min} value [4,20,26,27]. All physically realizable DRTs satisfy this cutoff condition because there is always a minimum relaxation time for the material considered [27,28]. However, such cutoff usually involves so small a value of τ_{min} that $\epsilon'_{C0}(\infty)$ is much smaller than one and $\epsilon'_{C1}(\infty)$ is only marginally larger than its $\epsilon_{C1\infty}$ no-cutoff value [4,26].

Therefore, in the present work, cutoff effects are ignored except in Section 5. Cutoff always leads to a nonzero plateau, $\sigma_{Ck}(\infty)$, as well, but most IS experimental data do not extend to high enough frequencies for this quantity to be estimated. Because $\epsilon_{C0\infty}$ is zero for the K0, we must form an equation similar to Eq. (8) by using $\epsilon_{C0}(0)$ instead. Then, the CSD0 results comparable to the CMF CSD1 ones above are [4,5,8]

$$M_{C0}(\omega) = i\omega\epsilon_V I_{C0}(\omega)/\sigma_0, \tag{12}$$

and

$$\sigma_0 = \epsilon_V\epsilon_{C0}(0)/\langle\tau\rangle_0 = \epsilon_V\epsilon_{C0}(0)/\tau_{o0}\langle x\rangle_0, \tag{13}$$

where data fitting leads to estimates of β_0 and τ_{o0} that differ from the estimates of $(1-\beta_1)$ and τ_{o1} obtained from fitting the same data with the K1 CMF model. Further, though $<x>_0$ and $<x>_{01}$ are calculated from the same K0 DRT, they are functions of β_0 and β_1, respectively, and so may be quite different in value.

Note that the use of the Eq. (11) SE temporal response in Eq. (2) leads to dispersed resistive, not dielectric, frequency response, and the resulting $\rho_{C1}(\omega) = \rho_0 I_1(\omega) = [1 - I_{C0}(\omega)]/\{i\omega\epsilon_V\epsilon_{C1\infty}\}$ expression is related, again through Eq. (2), to a distribution of resistivity relaxation times. For $\beta_0 = 0.5$, an analytical expression for $G_0(x)$ is known [23], so that one for $G_1(x)$ is also available. The τ_{o1} characteristic relaxation time of the CSD0 SE response of Eq. (11) is necessarily a conductive-system quantity unrelated to $\epsilon_{D\infty}$ since it is a part of pure conductive-system frequency response and is associated through Eq. (8) with only conductive-system quantities.

When a CSD0 or CSD1 DRT is a delta function, one obtains Debye-relaxation frequency response with $\beta_0 = 1$ or $\beta_1 = 0$ and $<x> = 1$, response involving a frequency-independent resistance and capacitance in parallel, both purely conductive-system quantities. The full response with $\epsilon_{D\infty}$ taken into account then involves two capacitances in parallel, represented at high frequency by $\epsilon_\infty = \epsilon_{C1\infty} + \epsilon_{D\infty}$. In contrast, the OMF result in this limit involves just $\epsilon_{D\infty}$ and leads to

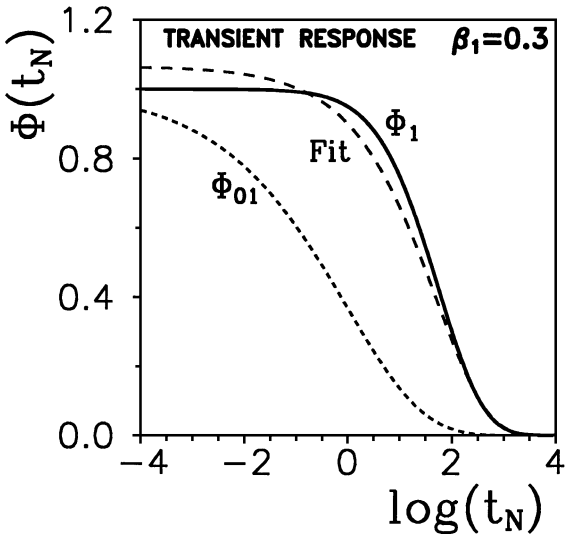

Fig. 2. Solid curve: accurate Φ_1 K1 temporal response for $\beta_1 = 0.3$. The "Fit" curve is the result of a weighted NLS fit of the Φ_1 data to the SE model, and the short-dash curve is ordinary SE response using the parameters that led to the Φ_1 curve. Here $t_N \equiv t/\tau_n$, with $\tau_n = 1$ s.

the Maxwell dielectric-material expression for τ_{OMF}, one that involves a resistance in parallel with a capacitance associated with $\epsilon_{D\infty}$, not the proper limit for CSD1 behavior. See also Section 6 below.

Clearly, CSD stretched-exponential temporal response does not include a term that could yield a part of the frequency response involving $\epsilon_{D\infty}$. One can obtain the temporal response from knowledge of the appropriate DRT [4,23,26]; therefore, from $G_1(x)$, a purely CSD quantity, we can calculate the associated $\Phi_1(t)$. As one might expect, it turns out that $\Phi_1(t)$ is not of stretched-exponential character [26,27]. Fig. 2 shows some results for $R=1$, $\tau_{o1}=1$ s, and $\beta_1=0.3$. When the $\Phi_1(t)$ K1 response was fitted by the K0 SE using LEVM with proportional weighting, the curve marked "Fit" was obtained. Although appreciable differences from the Φ_1 curve are apparent, they would be much less obvious in a log–log plot. The actual fit led to a value of S_F, the relative standard deviation of the fit residuals, of about 8%, and to poor R, τ_o, and β_1 estimates of about 1.07, 52 s, and 0.45. Similar poor results were found when the exact data fitted involved the $\beta_1=0.5$ choice.

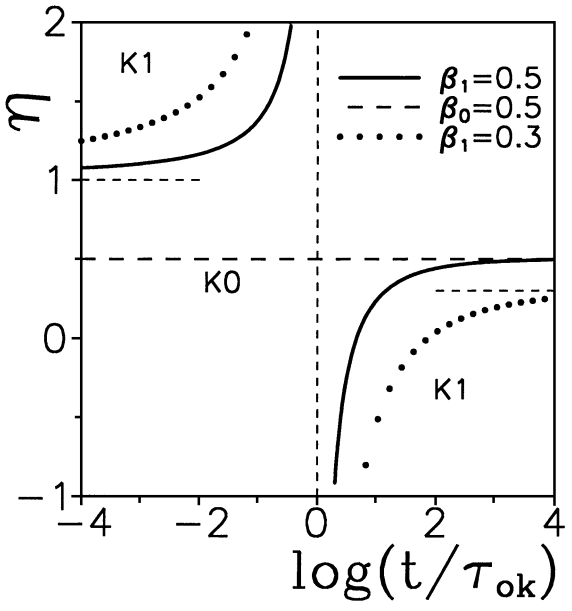

Fig. 3. Plots of $\eta \equiv \log[-\ln(\Phi_k(t))]/\log(t/\tau_{ok})$ for Φ_1 and Φ_0 with two different values of β, demonstrating that $\Phi_1(t)$ is not of SE character while $\Phi_0(t)$ is.

There is a more sensitive way to evaluate the appropriateness of representing temporal response by the SE when the value of τ_{ok} is known. Let $\eta \equiv \log[-\ln(\Phi_k(t))]/\log(t/\tau_{ok})$, a quantity equal to β_0 for all t when $\Phi_k(t)=\Phi_0(t)$ and is thus of SE character and $R=1$. Fig. 3 shows results for $\beta_1=0.3$ and 0.5, as well as $\beta_0=0.5$. The horizontal dashed lines indicate the asymptotic limits of the curves. Clearly, the K1 limits are approached faster the larger β_1.

4. Equality of corrected macroscopic and microscopic frequency-response models

4.1. Checking the CMF and STM isomorphism

Recently, Ngai and León [18] have stated that "The question of how to relate the macroscopic conductivity relaxation measurement. . .to the microscopic movement of ions is a problem that must be resolved." In two similar treatments [18,22], these authors showed that "the electric modulus (by which they meant the OMF) faithfully reproduces the shape of the dispersion of the microscopic ionic movement." To do so, they compared the frequency-response predictions of a slightly modified version of the macroscopic OMF with those of the 1973 continuous-time, random-walk, microscopic stochastic transport model (STM) of Scher and Lax [29]. Because there are several problems with these analyses, discussed below, it is worthwhile to show that corrected versions of both dispersed-relaxation models are isomorphic, thereby emphasizing the importance of the resulting joint model. Although a brief treatment of the matter has recently appeared [19], the importance of the subject merits a more complete analysis.

We shall first show how the above isomorphism may be established and then compare the results with the related but inappropriate ones of Ngai and León [18]. Although the joint model may involve different kinds of mobile charge, such as electrons or ions, we shall specialize here to an ionic situation where only cations are mobile, the usual case when the modulus formalism is used for the analysis of experimental frequency-response data from disordered ionic materials. Although there are many different expressions for the dc conductivity of a conducting system [30],

the usual Nernst–Einstein expression for this quantity when the fraction of available sites occupied by mobile charges is small, is [31,32]

$$\sigma_0 = [\gamma N(qd)^2/6kT]/\tau_H. \quad (14)$$

Here N is the total cation density; γ is the fraction of mobile cations; q is the cation charge; d is the RMS single-hop distance for a hopping ion, often designated as $[<r^2>]^{1/2}$; and τ_H is a thermally activated hopping time. It is related to the characteristic relaxation time of the response model, $\tau_o = \tau_a \exp(E_\tau/kT)$, where τ_a is temperature independent.

In terms of the present notation, the final STM expression for the complex conductivity for the CSD1 situation is [29]

$$\sigma_{STM}(\omega) = [\gamma N(qd)^2/6kT]\{i\omega I_{C0}(\omega)/\{1 - I_{C0}(\omega)\}\}, \quad (15)$$

whose $\omega \to 0$ limit is just

$$\sigma_{STM}(0) = [\gamma N(qd)^2/6kT]/\langle\tau\rangle_{01}, \quad (16)$$

where the τ_H, of Eq. (14) was identified by Scher and Lax as the mean waiting time for a hop and was calculated by using their equivalent of the first part of Eq. (4). Thus, this mean hop time is also the mean CMF relaxation time, $<\tau>_{01}$ [19]. If we set $\sigma_{STM}(0)$ equal to the σ_{01} of Eq. (8), we obtain the important result [8,19,33]

$$\epsilon_{C1\infty} = [\gamma N(qd)^2/6kT\epsilon_V], \quad (17)$$

indicating that when γ is temperature independent (the case of unassociated charge carriers), $\epsilon_{C1\infty}$ is proportional to $1/T$. Such dependence was approximately found from LEVM CMF K1 fitting of $Na_2O{\cdot}3SiO_2$ data [5], and very accurate $1/T$ dependence was recently established for $0.88ZrO_2{\cdot}0.12Y_2O_3$ data [33]. All CMF fitting carried out so far has shown that well-defined estimates of the values of both $\epsilon_{C\infty}$ and $\epsilon_{D\infty}$ may be obtained using CNLS data fitting with an appropriate CSD1 model, one which usually must contain electrode as well as bulk response parts [4–7,9,20,33,34]. Fits without a free or fixed separate $\epsilon_{D\infty}$ parameter, as with the OMF, were always considerably poorer than those when it was included and free to vary, as in the CMF. As discussed elsewhere [34], CMF fits are not superior to OMF ones just because they have one more free fitting parameter.

If we now use Eq. (17) in Eq. (15) and convert to the dielectric level, we obtain

$$\epsilon_{STM}(\omega) = \epsilon_{C1\infty}\{I_{C0}(\omega)/\{1 - I_{C0}(\omega)\}\}, \quad (18)$$

a result that differs from the macroscopic CMF expression for $\epsilon_{C1}(\omega)$ of Eq. (9) only by the presence of $I_{C0}(\omega)$ in the numerator of the latter, but not the former, equation. Thus, the Scher–Lax microscopic model as it stands is not quite isomorphic with the CMF one. It follows from Eqs. (9) and (18) that

$$\epsilon_{STM}(\omega) = \epsilon_{C1}(\omega) - \epsilon_{C1\infty}, \quad (19)$$

so it is only $\epsilon'_{STM}(\omega)$ that differs from $\epsilon'_{C1}(\omega)$, and the imaginary parts are identical. Unlike the CMF model involving K1, $\epsilon'_{STM}(\infty)$ is identically zero. Note that we have not specified a particular form for $I_{C0}(\omega)$ in the above expressions, but clearly the microscopic STM model is formally identical to the macroscopic CSD1 model except for the missing $\epsilon_{C1\infty} \neq 0$ term.

4.2. Proving the CMF and STM isomorphism, is $\epsilon'_{C1}(\infty)$ zero?

Although the above results do not fully establish the macro–micro isomorphism, that need not be the end of the matter. In private correspondence, Dr. Scher has noted that the STM is a low-frequency theory and thus its range of applicability does not necessarily extend to sufficiently high frequencies that a significant value of $\epsilon'_{STM}(\infty)$ can be obtained. Since a nonzero value does appear in the CSD1, and since the STM and CSD1 $\epsilon(\omega)$ imaginary parts are identical in form, it is reasonable to ask whether the $\epsilon'_{STM}(\omega)$ expression or the $\epsilon'_{C1}(\omega)$ one is fully consistent with the joint $\epsilon''(\omega)$ response. Unfortunately, the Kronig–Kramers relations cannot help answer this question because they only connect $\{\epsilon'_{STM}(\omega) - \epsilon'_{STM}(\infty)\}$ and $\epsilon''_{STM}(\omega)$. Thus, they cannot distinguish between a zero or a nonzero value of $\epsilon'_{STM}(\infty)$ using only $\epsilon''_{STM}(\omega)$ results.

But all is not lost! The above question may be answered using a CSD1 DRT approach and testing whether K1 $\epsilon''_{C1}(\omega)$ response alone leads to $\epsilon'_{C1}(\omega)$ response with a nonzero value of $\epsilon_{C1\infty}$. Let us start

with accurately calculated K1 frequency response extending over the range $0.01 \le \omega \le 10^8$ r/s. Parameter values were $\rho_0 = 10^9\ \Omega$ cm, $\tau_o = 5 \times 10^{-5}$ s, and $\beta_1 = 1/3$, and they led to $\epsilon_{C1\infty} \simeq 3.388$. The present β_1 value was selected for two reasons: first, many CMF data fits lead to a value near 1/3, virtually independent of temperature, ionic concentration, and material [8,9,33,34], and second, 1/3 is one of the few values of β_1 for which an analytical expression for the K1 DRT is known and incorporated in LEVM. Therefore, for the present β_1 choice, DRT inversion estimates may be compared to the exact DRT expression, more accurate than the separate DRT fitting model in LEVM appropriate for any plausible β_1 value.

We first used the inversion facility of LEVM to estimate the CSD1 DRT from both the complex $\epsilon_{C1}(\omega)$ and the $\epsilon''_{C1}(\omega)$ synthetic data sets. Such estimation assumed that the DRT was continuous and approximated it by 19 $\{C_i, \tau_i\}$ discrete points [17,26]. The fits were very good, with S_F values of 3.13×10^{-5} and 1.96×10^{-5}, respectively. Fig. 4 shows the estimated K1 DRT points and, for comparison, accurate K0 DRT curves for two values of β_0. Note that the K0 DRT curves are not those for the $G_0(x)$ distribution of Eq. (2) but are those following

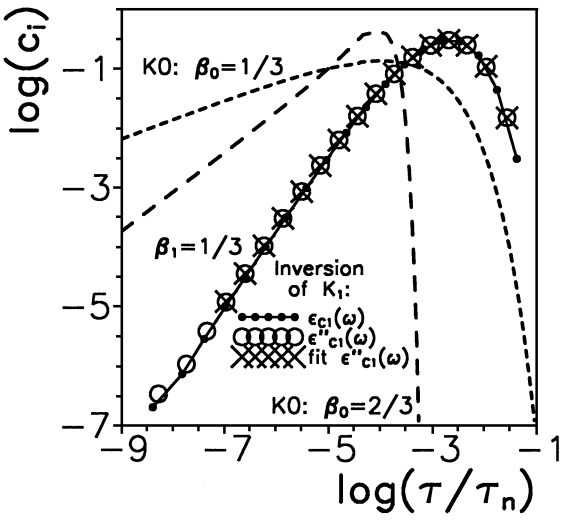

Fig. 4. Dashed lines: accurate distributions of conductive-system relaxation times for the K0 model with two different β_0 values. Solid line and symbols: estimates of K1-model distributions obtained by inversion of frequency-response data involving $\beta_1 = 1/3$.

when the integral is transformed to involve the logarithmic variable $y \equiv \ln(\tau/\tau_o) = \ln(x)$ [4,23,27]. The resulting distribution, $F_0(y)$ is just $xG_0(x)$, thus proportional to $G_1(x)$. Finally, $F_1(y)$ is given by $xG_1(x)$ and corresponds to the curve with solid circular points in the figure, a DRT derived directly from the full $\epsilon_{C1}(\omega)$ data. Points calculated for the $F_0(y)$ distribution are improperly identified as $G_0(x)$ ones in Ref. [13]. The figure shows that the small-τ region of the DRTs involves a power-law exponent of β_0 for the K0 and $(1+\beta_1)$ for the K1.

It is well known that DRTs derived from finite-range data yield somewhat inaccurate values for the last few smallest-τ points [26]. To provide a reference situation, fitting of the DRT points derived from the full *complex* $\epsilon_{C1}(\omega)$ data led to an appreciable S_F value of 0.079, but only the lowest-τ point showed a visible discrepancy on the log–log plot (not shown here). When fitting was carried out with the three lowest-τ points eliminated, the S_F value was 0.014, but parameter estimates were little changed. Fig. 4 includes points obtained by fitting the $\epsilon''_{C1}(\omega)$ DRT values with all 19 points and also with only the higher-τ 16 ones. The S_F values dropped from 0.081 to 0.0089 for the 19- and 16-point fits, respectively, but the estimated parameter values again did not change appreciably. For the 16-point fit they were $\tau_o \simeq 4.2 \times 10^{-5}$ s, and $\beta_1 \simeq 0.326$.

Next, the 19-point $\epsilon''_{C1}(\omega)$ DRT estimates were used in LEVM to calculate the corresponding full $\epsilon_{C1}(\omega)$ K1 frequency response by numerical integration of an equation corresponding to the present Eq. (2) [17,26]. The solid line in Fig. 5 is that of the original K1 $\epsilon'_{C1}(\omega)$ simulated data. In addition, the figure includes a curve of the DRT-derived $\epsilon'_{C1}(\omega)$ data and one showing the fit of that curve to the K1 model. Fitting of the derived $\epsilon_{C1}(\omega)$ complex, imaginary, and real parts to K1 led to all β_1 estimates of 0.333333 or better. The S_F, ρ_0, τ_o, and $\epsilon_{C1\infty}$ estimates were: (a) 0.022, 9.939×10^8, 4.81×10^{-5}, 3.281; (b) 0.0003, 9.9997×10^8, 4.997×10^{-5}, 3.387; and (c) 0.026, 9.957×10^8, 4.80×10^{-5}, and 3.268, respectively, with usual units. It is not surprising that the $\epsilon''_{C1}(\omega)$ fit results, derived directly from the $\epsilon''_{C1}(\omega)$ DRT estimate, are nearly exact. Note that for the present data, $\epsilon_{C10} = 10\epsilon_{C1\infty}$, and so the $\epsilon'_{C1}(\omega)$ results derived from the $\epsilon''_{C1}(\omega)$ DRT involve a value of $\epsilon_{C10} = 32.68$. On the present linear scale, this value

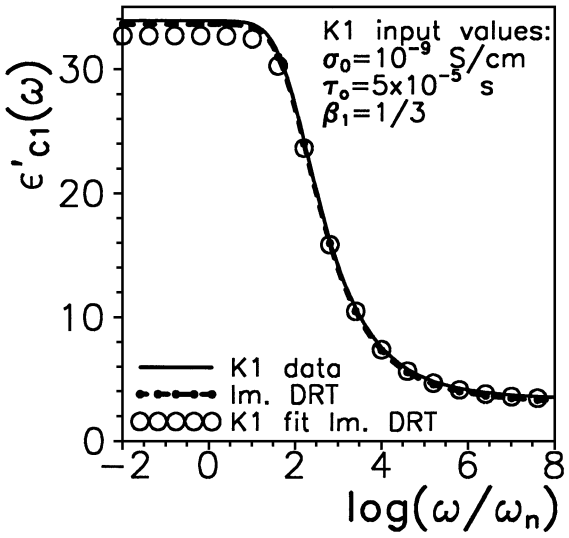

Fig. 5. Exact $\epsilon'_{C1}(\omega)$ data associated with the K1 DRT of Fig. 4 compared to the data set designated "Im. DRT" derived using the DRT obtained by inversion of accurate $\epsilon''_{C1}(\omega)$ data only. Also included are the results of fitting the estimated "Im. DRT" $\epsilon'_{C1}(\omega)$ results to the exact ones.

appears less accurate than the corresponding $\epsilon_{C1\infty}$ value but the relative errors are the same.

The most important result here is that the $\epsilon'_{C1}(\omega)$ points in the figure and the above fit results, all generated solely from the original $\epsilon''_{C1}(\omega)$ data, show reasonable values of the parameters and unequivocally establish that the derived value of $\epsilon'_{C1}(\infty)$ is nonzero and close to the input value. Therefore, the extended, consistent version of the STM, which includes $\epsilon_{C1\infty}$, should replace the original version, and the present results confirm that the extended STM and the CSD1 general response models are fully isomorphic. An important consequence of such isomorphism is that since the STM involves no explicit Coulomb interactions and the CSD1 model fits a large amount of data very well, such interactions may be of negligible importance for ordinary conductive-system data.

Finally, it is worth mentioning that a reviewer of the present manuscript pointed out that the "most severe error" in it is that $\epsilon'_{C1}(\infty)$ "has to be zero" but is not! We have seen that it is not zero in the OMF, the CMF, and the extended STM models, but, as mentioned in earlier work [8], since $\epsilon'_{C1}(\omega)$ and $\epsilon_{C1\infty}$ are entirely associated with mobile charges, $\epsilon'_{C1}(\omega)$ must eventually approach zero at very high frequencies if only because of the inertia of these charges. See also the results in Section 5 below.

Nevertheless, data and data analysis indicate that there is usually an appreciable high-frequency plateau region where $\epsilon'_{C1}(\omega) \simeq \epsilon_{C1\infty}$. For example, low-temperature CKN data shows a plateau in ϵ'_{dat} near $\nu = 10^{10}$ Hz and a slow decrease up to about $10^{11.5}$ Hz, the highest frequency shown [35]. Using a combination of dielectric and IR reflectivity measurements of sodium trisilicate, Cole and Tombari [36] found an approximate ϵ'_{dat} plateau apparently extending over four decades or more and then dropping from a value of about 8 down to 4 at about 10^{13} Hz. Although these results do not separate out $\epsilon_{C1\infty}$ and $\epsilon_{D\infty}$ contributions, CMF fits of data for several different glasses, which do lead to such separation [5,7–9,20,33,34], indicate that a nonzero $\epsilon_{C1\infty}$ is indeed needed, in addition to a separate $\epsilon_{D\infty}$ parameter, to obtain excellent fits.

4.3. Problems with the Ngai–León isomorphism

Ngai and León have followed a different approach to try to establish an isomorphism between the OMF model and the uncorrected STM [18,22]. Again, in terms of the present notation, they transform the OMF result of Eq. (5) to the complex admittance level and write the result in the form

$$\sigma_{OMF}(\omega) = i\omega\epsilon_V\epsilon_{D\infty}\left[\left\{1/\{1 - I_{C0}(\omega)\} - 1\right\} + 1\right], \tag{20}$$

where I have replaced their ϵ_∞ symbol by $\epsilon_{D\infty}$. They then rewrite Eq. (20) as $\sigma_{OMF}(\omega) = \sigma_{ion}(\omega) + i\omega\epsilon_V\epsilon_{D\infty}$, consistent with the philosophy that the OMF already contains all $\epsilon_{D\infty}$ effects. Ngai and León state that $\sigma_{ion}(\omega)$ is due only to the ionic diffusion. This quantity is given by

$$\sigma_{ion}(\omega) = \epsilon_V\epsilon_{D\infty}\left\{i\omega I_{C0}(\omega)/\{1 - I_{C0}(\omega)\}\right\}, \tag{21}$$

and is then compared with the STM result of Eq. (15).

Although the frequency-response term in the large braces of Eq. (21) is the same in form as that of Eq. (15), establishing a shape isomorphism, these authors understandably do not present an equation comparable to Eq. (17) above with $\epsilon_{C1\infty}$ there replaced by $\epsilon_{D\infty}$, one that would clearly be incorrect. Instead, they show

that equality of the dc conductivities leads in their case to

$$\tau_{\mathrm{OMF}}/\tau_{\mathrm{STM}} = [\gamma N(qd)^2/6kT\epsilon_{\mathrm{V}}\epsilon_{\mathrm{D}\infty}], \qquad (22)$$

a ratio that becomes unity when rewritten for the CMF approach with $\epsilon_{\mathrm{D}\infty}$ replaced by $\epsilon_{\mathrm{C1}\infty}$.

What are the problems with the Ngai/León approach? First, they do not point out that because their analysis requires the presence of $\epsilon_{\mathrm{D}\infty}$ in their $\sigma_{\mathrm{OMF}}(\omega)$ expression, a pure dielectric factor is introduced into a conductive-system result, one which, in the work of Scher and Lax [29] and other microscopic treatments, includes no such mixed-process elements. An instance of the same problem is evident in Eq. (21): Since it includes $\epsilon_{\mathrm{D}\infty}$ (or ϵ_∞), it is difficult to see how $\sigma_{\mathrm{ion}}(\omega)$ arises only from ionic diffusion as claimed. Finally, Ngai and León apparently did not note that the original STM frequency-response expression is not of exactly the same form as the macroscopic CSD1 model, as discussed in detail in the preceding section. Therefore, their shape isomorphism is established in reference to an inappropriate result and should be discounted even if there were no other problems with the analysis.

5. Some very-high-frequency effects: $\rho_{\mathrm{C1}\infty} \neq 0$ and DRT cutoffs

A reviewer of the original version of this work stated that the usual $\rho_{\mathrm{C1}\infty} = 0$ choice, an implicit part of all OMF analyses and an explicit one for most CMF ones, is contrary to physical reality because "*all* hopping models yield *finite* high-frequency conductivities." Interestingly, we also find in Ref. [37] the statement, "High-frequency plateau...are produced by all hopping models..." Physical reality indeed requires that all $\sigma'(\omega)$ data must reach a plateau value at sufficiently high frequencies; call it σ'_∞ [27,28].

The $\rho_{\mathrm{C1}\infty} = 0$ choice, whose inclusion was cited as one reason for recommending rejection of the manuscript, is, in fact, frequently plausible because, as discussed below, a physically reasonable nonzero $\rho_{\mathrm{C1}\infty}$ value will generally lead to effects at frequencies beyond those usually available in electrical measurements, and also because there is another intrinsic physical limitation that yields a high-frequency plateau in $\sigma'(\omega)$, whether $\rho_{\mathrm{C1}\infty}$ is zero or not. This limitation arises from the cutoff model [26,27], an improvement and generalization of the Ngai coupling model (see many references listed in Ref. [27] and some discussion in Ref. [38]). The cutoff model, as mentioned earlier, involves cutoff of the conductive-system DRT at a small value of τ. Further, Scher and Lax [29,p,4497], in discussing limitations of their 1973 STM approach, mention that the model does not, but should, include a maximum transition rate, thus introducing cutoff.

Since the question of the appropriateness of including a nonzero $\rho_{\mathrm{C1}\infty}$ in a response model has been raised, it is important to illustrate some of the consequences of doing so. To begin, let us rewrite Eq. (1) for $k=1$ as $\rho_{\mathrm{C1}}(\omega) = \rho_{\mathrm{C1}\infty} + \Delta\rho I_1(\omega)$, where $\Delta\rho \equiv (\rho_0 - \rho_{\mathrm{C1}\infty})$. Fig. 6 shows how nonzero $\rho_{\mathrm{C1}\infty}$ values can lead to a rapid decrease towards zero of $\epsilon_{\mathrm{C1}}(\omega)$ in the region where the constant $\epsilon_{\mathrm{C1}\infty}$ limit would otherwise be approached. In this region, it can be shown that the presence of $\rho_{\mathrm{C1}\infty}$ leads, on using Eqs. (1) and (9), to

$$\epsilon'_{\mathrm{C1}}(\omega) \simeq \epsilon_{\mathrm{C1}\infty}/\{1 + (\omega\rho_{\mathrm{C1}\infty}\epsilon_{\mathrm{V}}\epsilon_{\mathrm{C1}\infty})^2\}, \qquad (23)$$

showing that the decrease becomes proportional to ω^{-2}. This high-frequency-limiting response is of Debye form with a single temperature-dependent relaxation time, $\rho_{\mathrm{C1}\infty} \equiv \rho_{\mathrm{C1}\infty}\epsilon_{\mathrm{V}}\epsilon_{\mathrm{C1}\infty}$.

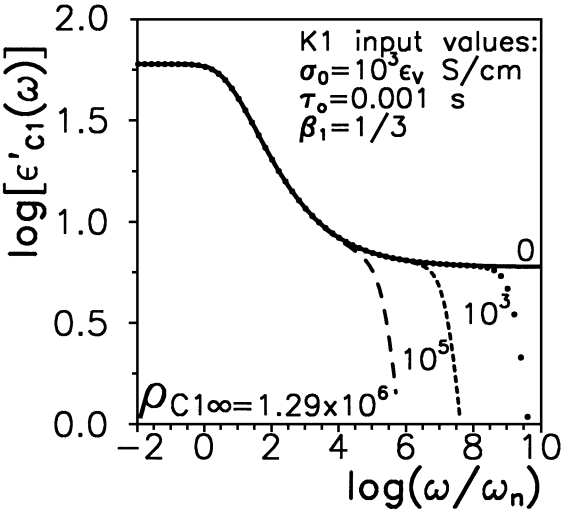

Fig. 6. Log–log plots of exact $\epsilon'_{\mathrm{C1}}(\omega)$ frequency response for four values of $\rho_{\mathrm{C1}\infty}$.

When $\rho_{C1\infty}$ is nonzero, one should properly change all $\rho_{C1\infty}=0$ ρ_0 and σ_0 symbols above to $\Delta\rho$ and $1/\Delta\rho$, respectively. But, as the results of Fig. 6 show, it is necessary that $\rho_{C1\infty}/\rho_0$ be considerably less than 10^{-4} before an appreciable frequency range appears where $\epsilon'_{C1}(\omega)$ approximates the $\epsilon_{C1\infty}$ results of Eq. (8), appropriate when $\rho_{C1\infty}=0$. As discussed below, it is likely that $\rho_{C1\infty}$ will generally be so small that this condition will be satisfied. Therefore, even when $\rho_{C1\infty}\neq 0$, for most conditions, there will be negligible difference between ρ_0 and $\Delta\rho$. Then, the use of Eq. (8) will remain appropriate and useful over a limited frequency range.

There is some plausible theoretical evidence based on the assumption of an exponential distribution of transition rates, that $\rho_{C1\infty}$ may be of the order of $\lambda\equiv\tau_a\epsilon_V$ or possibly $\lambda E_\tau/kT$ [38, Eqs. (B27), (B11)], with λ clearly temperature independent. Experimental results for several different materials [39] suggest that τ_a is likely to fall in the range of 10^{-14} to 10^{-17} s. It also appears that σ'_∞ does not exceed about 10 S/cm [37,40,41]. If this value of σ'_∞ were set equal to λ, one would obtain a minimum estimate of τ_a of about 10^{-14} s and a minimum value of $\tau_{C1\infty}$ of about 10^{-13} s for $\epsilon_{C1\infty}$ of the order of 10. Some non-activated temperature dependence is present in the above expression for $\epsilon'_{C1}(\omega)$, both from that of $\epsilon_{C1\infty}$, as in Eq. (17), and from the second form above of $\rho_{C1\infty}$ when it applies. The present expression for $\tau_{C1\infty}$ is similar to, but crucially different from, a relation presented in Ref. [41], Eq. (17), for the mismatch-and-relaxation model.

Fig. 7 shows $\rho_{C1\infty}$ effects on $\sigma'_{C1}(\omega)$ response. It is clear that nonzero $\rho_{C1\infty}$ leads to a finite-length power-law response region with a larger slope than that associated with ordinary CSD1 response, here $(1-\beta_1)=2/3$ for the K1 model. Such behavior has been illustrated previously for another response model [38], and it involves a slope value that approaches 2 as $\rho_{C1\infty}$ decreases, in full agreement with very-high-frequency results for several different materials [37,40,41]. In addition, the apparent limiting value of $T\sigma'_\infty$, which may be modeled by $T/\rho_{C1\infty}$, shows only a small, nonactivated increase with increasing temperature [37], in qualitative agreement with either of the above forms of $\rho_{C1\infty}$. In contrast, no theoretical expression for this quantity was discussed in Refs. [37,40,41]. In the high-slope region associated with

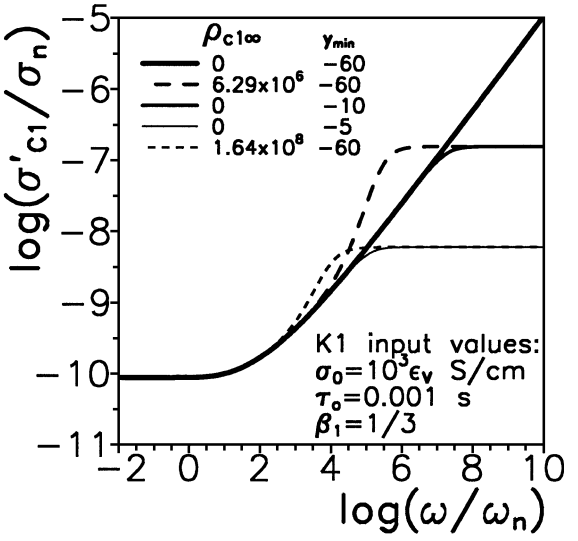

Fig. 7. Log–log plots of exact K1 $\sigma'_{C1}(\omega)$ frequency response for several values of $\rho_{C1\infty}$ and of the cutoff parameter y_{min}.

nonzero $\rho_{C1\infty}$, the response is again of Debye type and may be expressed as

$$\sigma'_{C1}(\omega)\simeq\epsilon_V\epsilon_{C1\infty}\tau_{C1\infty}\omega^2/\{1+(\omega\tau_{C1\infty})^2\}, \qquad (24)$$

where $\tau_{C1\infty}$ is defined above. Both the Ngai coupling model and the cutoff model also lead to limiting high-frequency Debye response of this type [27].

From recent measurements on an argyrodite compound up to a maximum frequency of 6 THz [42], the authors found that at high frequencies, fitting of their $\sigma'_{dat}(\omega)$ measurements required a term proportional to ω^2, identified as modeling the low-frequency flank of the silver vibrational contribution, consonant with the presence of a nonzero $\rho_{C1\infty}$. No plateau appeared up to the highest frequency shown, about 10^{11} Hz. It is worth noting, however, that high-frequency electrode or interface polarization can also lead to a slope approaching two and even to an apparent plateau [9,34].

Fig. 7 also shows separate cutoff-model results for $\rho_{C1\infty}$. When the DRT integral in Eq. (2) is transformed to involve the logarithmic variable y, and the bottom limit of the integral is set to $y_{min}=\ln(x_{min})=\ln(\tau_{min}/\tau_o)$ rather than to $-\infty$, the DRT is cut off at τ_{min} and is zero below this value [27]. The value $y_{min}=-60$, corresponding to $x_{min}\approx 10^{-26}$, is used here as the no-cutoff condition. When $y_{min}=-10$,

$x_{min} \simeq 4.5 \times 10^{-5}$, leading to $\tau_{min} \simeq 4.5 \times 10^{-8}$ s for the present situation. Incidentally, the nonzero values of $\rho_{C1\infty}$ shown in Fig. 7 were selected just to make the resulting $\sigma_{C1\infty}$ values equal to the $y_{min} = -5$ and -10 plateau values. These cutoff values will be designated as $(\sigma_{C1\infty})_{CO}$ to distinguish them from $\sigma_{C1\infty}$ values associated with $\rho_{C1\infty}$. As already mentioned, nonzero values of $(\sigma_{C1\infty})_{CO}$ do not lead to a nonzero $\rho_{C1\infty}$ value.

The most obvious difference in the curves arising from the two different processes is the extra high-slope region intrinsic to the presence of nonzero $\rho_{C1\infty}$. This difference usually allows one to distinguish between the two disparate causes of a σ'_∞ plateau. It is worth mentioning that the Ngai coupling model leads to results similar to those of the cutoff approach [27], and the Funke mismatch-and-relaxation model [37,41], one which has not been fitted to many different data sets, appears to yield shape response closer to that of the cutoff model than to that arising from a nonzero $\rho_{C1\infty}$ [43]. Some apparent defects in the Funke model are discussed in Ref. [43], and some aspects of the coupling model and several other response models are summarized in Ref. [39].

Finally, one always expects cutoff response to be present at sufficiently high frequencies, and, when $\rho_{C1\infty}$ is nonzero as well and $\sigma_{C1\infty} \gg (\sigma_{C1\infty})_{CO}$, one should find that when the ω^2 part of the response associated with $\rho_{C1\infty}$ is removed from the data, a $(\sigma_{C1\infty})_{CO}$ plateau appears that is associated only with the cutoff DRT of the basic conductive-system dispersion response, again consonant with experimental results and analysis [37,41]. The inclusion of both nonzero $\rho_{C1\infty}$ and y_{min} cutoff effects in a fitting model adds just two more free parameters to the model. With appropriate data, such fitting should allow one to estimate both $\rho_{C1\infty}$ and $(\sigma_{C1\infty})_{CO}$ values and to separate out their effects. Unfortunately, a request several years ago to Professor Funke for some of his very-high-frequency $\sigma'(\omega)$ data to implement such fitting met with no response.

6. Discussion and conclusions

The original modulus formalism modeling approach [11–13] was one of the first to discuss dispersed conductive-system response as opposed to its modeling in terms of a dispersed dielectric system. The appropriateness of this important approach was, I believe, weakened by its misidentification of the high-frequency-limiting dielectric constant associated only with mobile charge as either $\epsilon_{D\infty}$ or ϵ_∞, as discussed above and below. Here I summarize comparisons between the OMF and the CMF and their predictions for several different situations. The reader may then conclude which one seems to be the most appropriate. Because the OMF implicitly takes $\rho_{C1\infty} = 0$ the following comparisons are based on this assumption, but see Section 5 above for the effects of its inapplicability.

Consider first the Maxwell-relaxation-time expression

$$\tau_M = \epsilon_V \epsilon_\infty / \sigma_0, \tag{25}$$

often used by those who improperly treat dispersed conductive-system response as a dispersed dielectric-response situation [44]. See Section 1.2 herein, Ref. [6], and the Appendix of Ref. [7] for further detailed discussion of this equation and the differences between the two dispersion processes. Eq. (25) arises from the parallel combination of an ideal capacitance, represented here by ϵ_∞, and an independent ideal resistance, represented by $1/\sigma_0$.

For the dielectric-dispersion situation, ϵ_∞ has its usual meaning, and σ_0 is a parallel leakage conductivity unrelated to the dispersion process. For DSD, there is a separate characteristic relaxation time, τ_D, that is unrelated to τ_M and is a crucial part of the dielectric dispersion whether σ_0 is present or not. Thus, it is not appropriate to equate τ_D and τ_M in this situation because if this were done, Eq. (25) would require change in τ_D as σ_0 changed.

A different problem is present when Eq. (25), or equations similar to it, are used in CSD situations and analyses. Compare the expression for τ_{OMF} in Eq. (6) with that for τ_M of Eq. (25). In Eq. (6), $\epsilon_s = \epsilon_{D\infty}$, and it is often set equal to σ_∞. Unlike the DSD situation, for conductive-system dispersion σ_0 and τ_o are directly linked as parts of the same dispersion process and involve essentially the same thermal activation energy [33,38]. Thus, for this situation it is plausible that an equation such as Eq. (6) should apply. Nevertheless, this equation is inapplicable to CSD situations

because of the presence in it of $\epsilon_{D\infty}$ or ϵ_∞ [4–6]. We are now ready to discuss several comparisons between aspects of the OMF and the CMF approaches.

(A) It is a fact that mobile charges lead to real-part frequency response at the dielectric level, here designated $\epsilon'_C(\omega)$, for which $\epsilon'_C(\infty)$ may or may not be zero [4–6]. It is nonzero for the K1 dispersion model, the basis of both the OMF and the CMF, and it is termed $\epsilon_{C1\infty}$. A crucial difference between the OMF and the CMF is the replacement of the OMF ϵ_s of Eq. (6) by the CMF $\epsilon_{C1\infty}$ of Eq. (8). Unlike Eq. (6), Eq. (8) properly involves only quantities associated with, and arising from, charge motion. Thus, the OMF erroneously identifies the CSD1 $\epsilon_{C1\infty}$ with a dielectric constant that completely or partially includes dipolar/vibratory bulk dielectric effects through $\epsilon_{D\infty}$. Such mixing of CSD and bulk dielectric effects means that the dielectric quantity ϵ_s is fully determined by the value of the CSD product $\sigma_{OMF0}\tau_{OMF}<x>_{OMF}$, inconsistent with physical reasonableness and with experimental results.

(B) The OMF approach leads to response that ignores the existence of $\epsilon_{C1\infty}$ and, with ϵ_s replaced by ϵ_∞, involves $\epsilon_{D\infty}=\epsilon_\infty$. Thus, in fitting data with this model, no extra free dielectric parameter is required. In contrast, for the CMF, $\epsilon_{C1\infty}$ is fully determined by the other parameters in Eq. (8) and is thus not a free parameter. But since the effects of a nonzero $\epsilon_{D\infty}$ appear in all frequency-response data, this quantity must be treated as a free fitting parameter. Then, $\epsilon_\infty=\epsilon_{C1\infty}+\epsilon_{D\infty}$, and data fitting yields estimates of both contributions to ϵ_∞ [4–8,33,34]. On the other hand, OMF ϵ_∞ parameter estimates are improperly interpreted as representing $\epsilon_{D\infty}$, while in fact they include both parts of the actual ϵ_∞.

(C) The OMF and CMF models are both of CSD1 character and have been used to determine model parameters by data fitting. In the OMF case, analysis of $M''(\omega)$ data has led to improper β_1 estimates, ones which are not of true CSD character because they are derived from data sets that include both $\epsilon_{C1\infty}$ and $\epsilon_{D\infty}$ effects [13,16,44,45]. Table 2 in Ref. [13], often used for β_1 estimation, is, in fact, appropriate only for pure CSD response [4,23] but it has generally been used in conjunction with original $M''(\omega)$ data rather than that from which $\epsilon_{D\infty}$ effects have been eliminated. Since CMF analysis already includes $\epsilon_{D\infty}$ as a free parameter, however, its β_1 estimates are properly those appropriate for the pure CSD fitting model.

(D) Since only data expressed at the $\sigma'(\omega)$ or $\epsilon''(\omega)$ levels do not involve much or any effects from $\epsilon_{D\infty}$, OMF and CMF fits at these levels are equivalent and should lead to the same proper estimates of β_1, for example. For the other six IS fitting possibilities, where $\epsilon_{D\infty}$ strongly affects the data, one should find very nearly the same CMF estimates as for the other two but quite different ones for OMF fits. Data fitting for several different materials completely verifies these conclusions and leads to variable $(\beta_1)_{OMF}$ values of the order of 0.5 and to $(\beta_1)_{CMF}$ values of about 1/3, virtually independent of temperature and ionic concentration [8,33,34]. The limiting slope of $n=1-(\beta_1)_{CMF}$ of about 2/3 agrees closely with results compiled in 1994 for many materials from power-law $\sigma'(\omega)$ fits, while the corresponding $(\beta_1)_{OMF}$ values listed range from 0.47 to 0.83 [46]. Incidentally, another compilation of β values for various alkali oxide concentrations does not make it entirely clear whether all those listed are from K0 fits or from OMF determinations [47], but the trend toward $\beta=1$ as the concentration decreases is in agreement with that found for $(\beta_1)_{OMF}$ [33].

(E) The present work shows that the imaginary part of the $\epsilon(\omega)$ response of the Scher–Lax STM microscopic model is given by a general expression identical in form to that of the modulus formalism, and the real part differs only by not including a nonzero high-frequency limit, $\epsilon'_{STM}(\infty)$. For the K1 macroscopic response model used in the modulus formalism approach, the limit is $\epsilon_{C1\infty}$. By using *only* the DRT associated with $\epsilon''_{C1}(\omega)=\epsilon''_{STM}(\omega)$ response, it is demonstrated that the derived $\epsilon'_{C1}(\omega)$ response does indeed include $\epsilon'_{C1\infty}$, thus verifying a complete isomorphism between the forms of the augmented STM and the CSD1. Since the OMF approach does not recognize the existence of $\epsilon_{C1\infty}$, it cannot be brought into full consonance with the augmented STM model.

(F) It has recently been demonstrated that nearly constant-loss effects are likely to be associated with an increase in $\epsilon_{D\infty}$ with increasing ionic concentration [33], one arising from interactions between mobile charges and their surroundings. The OMF approach does not and cannot lead to such detailed results.

Definitions of acronyms

CMF	corrected electric modulus formalism approach
CNLS	complex nonlinear least squares
CSD	conductive-system dispersion
CSD*k*	two types of CSD response with $k=0$ or 1
DRT	distribution of relaxation times, τ
DSD	dielectric-system dispersion
IS	immittance spectroscopy
KWW	Kohlrausch–Williams–Watts response model
KWW*k*	KWW response defined by index k, where $k=0$ or 1
K*k*	abbreviated form of KWW*k*
LEVM	the complex-nonlinear least-squares fitting program used herein
OMF	original electric modulus formalism approach
SE	stretched-exponential response; see Eq. (11)
STM	stochastic transport model of Scher and Lax

Acknowledgements

It is a pleasure to thank Dr. Carlos León for extensive correspondence that has helped me better understand many aspects of the original modulus-formalism dispersion model.

References

[1] J.R. Macdonald (Ed.), Impedance Spectroscopy–Emphasizing Solid Materials and Systems, Wiley-Interscience, New York, 1987.
[2] K.L. Ngai, R.W. Rendell, Phys. Rev., B 61 (2000) 9393.
[3] B.A. Boukamp, J.R. Macdonald, Solid State Ionics 74 (1994) 85.
[4] J.R. Macdonald, J. Non-Cryst. Solids 197 (1996) 83, erratum; J.R. Macdonald, J. Non-Cryst. Solids 204 (1996) 309. In addition, G_D in Eq. (A2) should be G_{CD}.
[5] J.R. Macdonald, J. Non-Cryst. Solids 212 (1997) 95, erratum; J.R. Macdonald, J. Non-Cryst. Solids 220 (1997) 107. In addition, Eq. (7) should only be applied when $0 \le \rho_{C\infty} \ll \rho_{C0}$. Finally, the symbol σ_o should be removed from the right end of Eq. (12) and "dx" should be moved from the left side of the term in square brackets in Eq. (A.5) to the right side.
[6] J.R. Macdonald, Braz. J. Phys. 29 (1999) 332. Available online at http://www.sbf.if.usp.br/WWW_pages/Journals/BJP/Vol.29/index.htm.
[7] J.R. Macdonald, Solid State Ionics 133 (2000) 79.
[8] J.R. Macdonald, J. Appl. Phys. 90 (2001) 153, Erratum: in Eq. (10), $\sigma_0\Gamma$ should be replaced by $\sigma_0\tau_o\Gamma$.
[9] J.R. Macdonald, J. Chem. Phys. 115 (2001) 6192.
[10] F.E.G. Henn, R.M. Buchanan, N. Jiang, D.A. Stevenson, Appl. Phys., A 60 (1995) 515.
[11] V. Provenzano, L.P. Boesch, V. Volterra, C.T. Moynihan, P.B. Macedo, J. Am. Ceram. Soc. 55 (1972) 492.
[12] P.B. Macedo, C.T. Moynihan, R. Bose, Phys. Chem. Glasses 13 (1972) 171.
[13] C.T. Moynihan, L.P. Boesch, N.L. Laberge, Phys. Chem. Glasses 14 (1973) 122.
[14] B. Roling, J. Non-Cryst. Solids 244 (1999) 34.
[15] I.M. Hodge, C.A. Angel, J. Chem. Phys. 67 (1977) 1647.
[16] C.T. Moynihan, J. Non-Cryst. Solids 172–174 (1994) 1395.
[17] J.R. Macdonald, L.D. Potter Jr., Solid State Ionics 23 (1987) 61, The new Version 7.11 of the comprehensive LEVM fitting program may be downloaded at no cost from http://www.physics.unc.edu/ ~ macd/. It includes an extensive manual, executable programs, and full source code. More information is provided about LEVM at this www address.
[18] K.L. Ngai, C. León, Phys. Rev., B 60 (1999) 9396.
[19] J.R. Macdonald, Phys. Rev., B 63 (2001) 052205.
[20] J.R. Macdonald, J. Appl. Phys. 82 (1997) 3962.
[21] I. Svare, F. Borsa, D.R. Torgeson, S.W. Martin, H.K. Patel, J. Non-Cryst. Solids 185 (1995) 297.
[22] K.L. Ngai, C. León, Solid State Ionics 125 (1999) 81.
[23] C.P. Lindsey, G.D. Patterson, J. Chem. Phys. 73 (1980) 3348.
[24] R. Kohlrausch, Pogg. Ann. Phys. Chem. 91 (2) (1854) 179.
[25] G. Williams, D.C. Watts, Trans. Faraday Soc. 66 (1970) 80.
[26] J.R. Macdonald, Inverse Problems 16 (2000) 1561; J.R. Macdonald, J. Comput. Phys. 157 (2000) 280.
[27] J.R. Macdonald, J. Appl. Phys. 84 (1998) 812, The word "out" in the third line from the bottom of the first column on p. 820 should be "but".
[28] J.R. Macdonald, Solid State Ionics 25 (1987) 271.
[29] H. Scher, M. Lax, Phys. Rev., B 7 (1973) 4491; M. Lax, H. Scher, Phys. Rev. Lett. 39 (1977) 781.
[30] A.S. Nowick, in: G.M. Murch, A.S. Nowick (Eds.), Diffusion in Crystalline Solids, Academic Press, Orlando, 1985, Chap. 3; A.S. Nowick, W.-K. Lee, H. Jain, Solid State Ionics 28–30 (1988) 89.
[31] H. Jain, J. Non-Cryst. Solids 66 (1984) 517.
[32] D.L. Sidebottom, Phys. Rev. Lett. 82 (1999) 3653.
[33] J.R. Macdonald, J. Chem. Phys. 116 (2002) 3401.
[34] J.R. Macdonald, J. Non-Cryst. Solids, in press.
[35] P. Lunkenheimer, A. Pimenov, A. Loidl, Phys. Rev. Lett. 78 (1997) 2995.
[36] R.H. Cole, E. Tombari, J. Non-Cryst. Solids 131–133 (1991) 969.
[37] K. Funke, B. Roling, M. Lange, Solid State Ionics 105 (1998) 195.
[38] J.R. Macdonald, Phys. Rev., B 49 (1994) 9428.
[39] A.S. Nowick, A.V. Vaysleyb, I. Kuskovsky, Phys. Rev., B 58 (1998) 8398.

[40] K. Funke, Solid State Ionics 94 (1997) 27.
[41] K. Funke, Z. Phys. Chem. 206 (1998) 101.
[42] R. Belin, A. Zerouale, A. Pradel, M. Ribes, Solid State Ionics 143 (2001) 445.
[43] J.R. Macdonald, Solid State Ionics 124 (1999) 1.
[44] C.T. Moynihan, J. Non-Cryst. Solids 203 (1996) 359.
[45] C.T. Moynihan, Solid State Ionics 105 (1998) 175.
[46] D.L. Sidebottom, P.F. Green, R.K. Brow, J. Non-Cryst. Solids 183 (1995) 151.
[47] K.L. Ngai, R.W. Rendell, Phys. Rev., B 40 (1989) 10550.